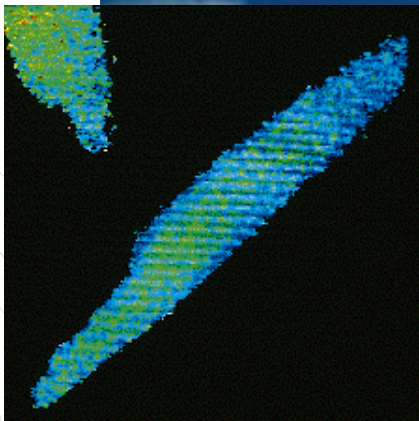


Edition Wissenschaft

Forschungsgemeinschaft Funk e.V. · G 14515 · Edition No. 2/E
Special edition in English · May 1998



Calcium Homeostasis of Isolated Heart Muscle Cells Exposed to Pulsed High-Frequency Electromagnetic Fields

S. Wolke, U. Neibig, R. Elsner, F. Gollnick,
and R. Meyer

Edition
Wissenschaft



Forschungsgemeinschaft Funk

Editorial

Dear Readers,

the study "The Influence of High-Frequency Electromagnetic Fields on the Intracellular Calcium Concentration of Excitable and Non-Excitable Cells" is part of a series of research projects carried out by the Forschungsverbund Braunschweig on "Biological Effects of High-Frequency Electromagnetic Fields" and was promoted by the Forschungsgemeinschaft Funk. The original study was published as "Edition Wissenschaft" No. 2 in 1995. The present issue of the study was published in 1996 as an off-print in the American journal "Bioelectromagnetics" focussing on the examination of heart muscle cells.

During the use of mobile phones the user is exposed to electromagnetic fields. In order to avoid health hazards, the manufacturers have to stick to certain regulations and norms. These norms are based largely on the knowledge of the thermal effects of electromagnetic fields. Within the framework of the research project it was examined whether electromagnetic fields might have athermal effects, too. It is useful and usual to observe such effects on the biological reaction of animal and human cells.

The present issue deals with the effects of pulsed high-frequency fields in the range between 900 and 1,800 MHz, as used for mobile telecommunications, on the intracellular calcium concentration, $[Ca^{2+}]_i$, in heart muscle cells. There was no evidence found that weak high-frequency electromagnetic fields have significant influence. Although this study cannot exclude effects, the authors state that such an influence is not very probable.

Gerd Friedrich

Content

Calcium Homeostasis of Isolated Heart Muscle Cells Exposed to Pulsed High-Frequency Electromagnetic Fields	3
1. Introduction	3
2. Materials and Methods	4
2.1 Cell Isolation	4
2.2 Experimental Setup and Measuring Principle	4
2.3 High-Frequency Exposure System	6
2.4 Dosimetry	6
2.5 Experimental Design and Tested Parameters	8
2.6 Evaluation Procedure	8
3. Results	9
4. Discussion	12
5. Acknowledgements	14
6. References	14

Calcium Homeostasis of Isolated Heart Muscle Cells Exposed to Pulsed High-Frequency Electromagnetic Fields

S. Wolke, U. Neibig, R. Elsner, F. Gollnick, and R. Meyer

Institut für Strahlen- und Kernphysik der Universität Bonn, Bonn, Federal Republic of Germany (S.W.);

Institut für Nachrichtentechnik Braunschweig, Braunschweig, Federal Republic of Germany (U.N., R.E.);

Physiologisches Institut der Universität Bonn, Bonn, Federal Republic of Germany (F.G., R.M.)

1. Introduction

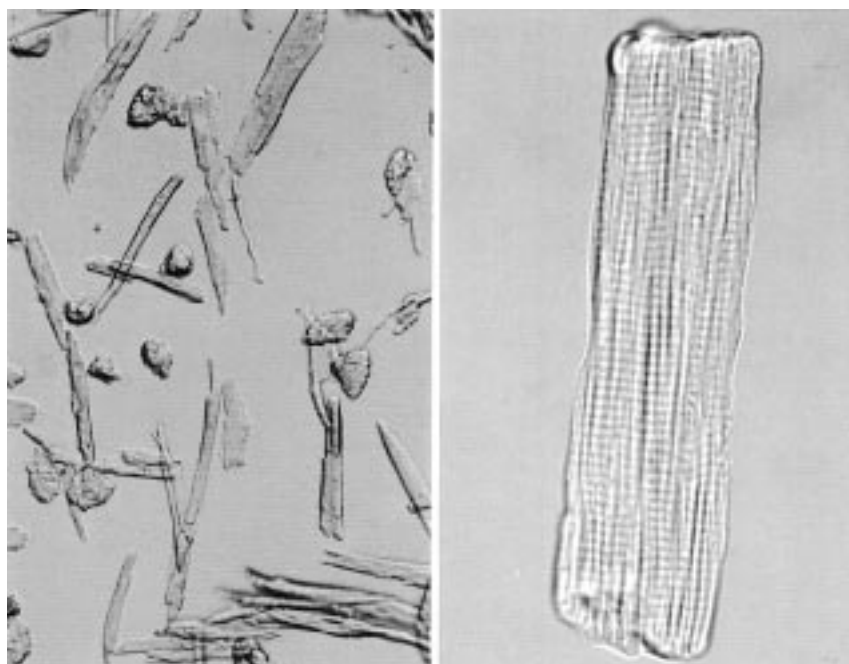
The intracellular calcium concentration ($[Ca^{2+}]_i$) plays an important role in the control of cell signaling and cellular events such as movement, contraction, or cell division [for reviews, see Carafoli, 1987; Berridge, 1993; Clapham, 1995]. If electromagnetic fields influence cellular activities, then this is probably reflected in the Ca^{2+} homeostasis of the cells. The $[Ca^{2+}]_i$ is influenced by the conductance of the cell membrane as well as the permeability of intracellular stores and the concentration of intracellular messengers such as inositol trisphosphate [for review, see Pozzan et al., 1994]. Such intracellular messengers depend on the activation of specific receptors in the membrane. Thus, measuring $[Ca^{2+}]_i$ will discern changes of many possible targets

of electromagnetic fields. An effect of high-frequency electromagnetic fields that is mediated by $[Ca^{2+}]_i$ has been demonstrated in atrial smooth muscle cells [Miura and Okada, 1991; Miura et al., 1993]. Application of high-frequency electromagnetic fields of 10 MHz modulated with 10 kHz increased the formation of nitric oxide, inducing an increase in the diameter of the arterioles. This mechanism is dependent on $[Ca^{2+}]_i$ [Blatter and Wier, 1994].

To test the influence of high-frequency fields on Ca^{2+} homeostasis, various $^{45}Ca^{2+}$ efflux studies on neuronal tissue and cells have been carried out since the first work of Bawin et al. [1975]. Carrier frequencies of 50 MHz [Blackman et al., 1980a, 1989], 147 MHz [Bawin et al., 1975], 450 MHz [Bawin et al., 1978], and 915 MHz [Dutta et al., 1984] modulated

with frequencies between 0 Hz and 30 Hz and 50 Hz have been applied. All of these studies have demonstrated an increase in $^{45}Ca^{2+}$ efflux at modulation frequencies around 16 Hz. This phenomenon does not seem to be restricted to neuronal cells; it was also reported for isolated frog hearts by Schwartz et al. [1990]. An influence of high-frequency electromagnetic fields on electrical parameters of the cell membrane, e.g., membrane potential [Kullnick, 1992] or membrane currents [Tarricone et al., 1993], has also been shown. Changes in these parameters are known to cause changes in $[Ca^{2+}]_i$ as well. However, direct measurements of $[Ca^{2+}]_i$ under the influence of modulated high-frequency fields have been lacking.

The aim of this study was to test whether the frequency and pulse



Light microscopic bright field shot of isolated heart muscle cells. On the left: Overall view with few circular destroyed cells and many stick-shaped vital cells. On the right: Detailed shot of an isolated heart muscle cell.

patterns emitted from modern digital wireless telecommunication devices (GSM standard) influence the $[Ca^{2+}]_i$ in excitable cells under athermal exposure conditions. Other pulse patterns that are near the “frequency windows” demonstrated in efflux studies were also included in the study to see whether there is an influence on the $[Ca^{2+}]_i$ in these cases. Isolated heart muscle cells of the guinea pig were chosen as a cell model for two reasons. 1) These cells express numerous elements of Ca^{2+} homeostasis, such as Ca^{2+} channels in the cell membrane, intracellular Ca^{2+} stores, various hormone receptors, and a number of Ca^{2+} transport mechanisms. 2) There are divergent results reported in the literature obtained with heart cells. Schwartz et al. [1990] reported an increased $^{45}Ca^{2+}$ efflux

from whole frog hearts in the presence of 240 MHz field pulsed at 16 Hz. This finding was not reproduced in a second report on $^{45}Ca^{2+}$ efflux from isolated frog atrial trabeculae exposed to 1 GHz fields of continuous waves and pulsed at 0.5 and 16 Hz [Schwartz and Mealing, 1993].

2. Materials and Methods

2.1 Cell Isolation

Myocytes from adult guinea pig ventricles were isolated by retrograde perfusion of the excised heart in a Langendorff apparatus. Cells were separated by perfusion with trypsin and collagenase in 130 mM potassium glutamate as

proposed by Achenbach et al. [1985]. An exact description of the procedure is given by Stegmann et al. [1990]. The Tyrode's solution that was used as a standard solution during the isolation procedure and the experiments had the following composition (in mM): NaCl, 135; KCl, 4; $CaCl_2$, 1.8; $MgCl_2$, 1; glucose, 11; HEPES, 2 (pH 7.2 with NaOH); bovine serum albumin, 1 g/liter. After the isolation, the cells could be kept in Tyrode's solution saturated with O_2 , for up to 5 h without visible changes. To adjust the membrane potential of the cells to different values, the K^+ and Na^+ concentrations of the standard solution were varied according to Nernst's equation (see Table 3).

2.2 Experimental Setup and Measuring Principle

The $[Ca^{2+}]_i$ was measured by means of quantitative image analysis with the fluorescent Ca^{2+} indicator dye fura-2 [Grynkiewicz et al., 1985]. With increasing Ca^{2+} concentration $[Ca^{2+}]_i$, excitation light of 340 nm leads to an increasing emission at 510 nm, and excitation light of 380 nm leads to a decreasing emission at 510 nm. Therefore, the ratio of the 340 nm and 380 nm signals is an indicator for $[Ca^{2+}]_i$. By comparison of the measured ratio values to those from solutions with known $[Ca^{2+}]_i$, the system can be calibrated. We used solutions of seven $[Ca^{2+}]_i$ (pCa = 3, 4, 5, 6, 7, 8, 9) in rectangular glass capillaries 50 μm high and 600 μm wide. The calibration solution was made to resemble the ionic conditions of the cytoplasm (in mM): K^+ , 135; Na^+ , 5; Cl^- , 122.5–140.0 depending on the desired $[Ca^{2+}]_i$; HEPES, 10;

EGTA, 10; fura-2 salt, 10–25 μM . The amount of Ca^{2+} and Mg^{2+} that had to be added to give the desired free $[\text{Ca}^{2+}]$ was calculated using the computer program of Fabiato [1988]. Because the optical path length in the capillary is about five times the thickness of a cell, a concentration of fura-2 that is five times smaller is needed in the capillary to gain the same brightness as the cell's fluorescence. By comparing the original fluorescence images (elicited by 340 and 380 nm light) of a capillary to those of a resting cell, the difference in brightness could be detected. To correct for this difference, the fura-2 concentration in the capillaries was adapted to the brightness emitted by an unstimulated single cell during an experiment. This was done by mixing calibration solutions with or without fura-2 but of the same pCa. The fura-2 concentration determined by this procedure was used in each of the seven calibration solutions. Each of the seven solutions was filled into a separate capillary. Each capillary was imaged at exactly the same settings of the image analysis system that were used in the experiment. The measured ratio values were fitted with a sigmoidal function, which then served as a calibration curve. Calibrations carried out in this way usually revealed K_d values around 400 nM.

The cells were loaded with the membrane permeant fura-2/AM [Grynkiewicz et al., 1985]. An appropriate amount of fura-2 was loaded into the heart muscle cells by incubation for 15 min at 37 °C in 1 μM fura-2/AM dissolved in standard medium.

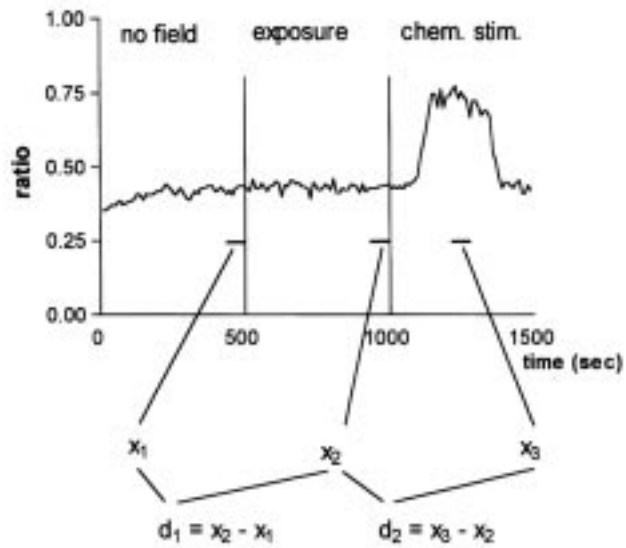


Fig. 1. Design of the experiments. Ratio of one cell plotted vs. the time. The experiment consists of three phases: I (without field), II (exposure), and III (without field but with chemical stimulation). The exposure period (900 MHz carrier frequency, 217 Hz pulsation frequency) is indicated by two vertical lines. The reversible effect of chemical stimulation is visible during the third phase. The three characteristic ratio values x_1 , x_2 , and x_3 are gained by averaging ten ratio values during the time periods marked in the graph. The differences d_1 and d_2 between the x values represent the influence of the electromagnetic field (d_1) and the effect of the chemical stimulation (d_2).

The experimental setup was based on an inverted microscope (Zeiss IM 35) with epifluorescence illumination. The microscope is mounted on a shock-absorbing working platform. An image analysis system consisting of an intensified CCD camera (Hamamatsu C 2400-77H) and the Hamamatsu Intracellular Ion Measurement System (ICMS, ver. 4.1) was used to detect and to measure the fluorescence light. Part of the Hamamatsu ICMS is a PC equipped with a Matrox MVP-AT frame grabber. This PC controls a step motor-driven filter changer with 340/10 and 380/10 nm band-pass filters and a shutter that are inserted in the epifluorescence beam path. A more detailed description of the calibration procedure and the setup can be found in Gollnick et al. [1991].

Using a $\times 16$ objective (Zeiss Neofluar $\times 16$; numerical aperture, 0.50) or a $\times 32$ objective (Zeiss Ultrafluor $\times 32$; numerical aperture, 0.40), up to 30 cells can be visualized simultaneously. Images were digitized on line in a 256×256 pixel array with 256 gray levels. Every 10 s (for long-term exposure, every 60 s), four images at 340 nm and four images at 380 nm were averaged. The averaged images were stored, and the ratio was calculated for each pixel. For evaluation of the time course of the $[\text{Ca}^{2+}]_i$, a measurement window was placed on each cell. The size of each window was chosen to be smaller than the outline of the cell onto which it was projected. All living cells (cells with bricklike shape) visible in the image were selected. Average ratio or concentration for all

pixels in window calculated and plotted vs. time (see Fig. 1).

2.3 High-Frequency Exposure System

The exposure system consisted of a cubic transversal-electromagnetic (TEM) cell with a 7 cm edge length and a usable frequency range up to 2 GHz connected to a UHF power-signal generator (SLRD BN 41004/50; Rohde and Schwarz, Munich, Federal Republic of Germany) with the facility for external modulation (rectangular; modulation up to 100%). The spectral width of the high-frequency signal was 3.6 kHz at 900 MHz measured with a spectrum analyzer (Tektronix 2710). The rise and fall time of the square-wave modulation signal was 2.5 μ s. Using an input power of 1 W, the power density at the bottom of the empty TEM cell was 76.2 W/m² (see Table 1).

Inside the TEM cell, there is an open experimental chamber with a volume of 200 μ l filled with the cell suspension. The experimental chamber is equipped with facilities for perfusion and temperature control (Fig. 2). Temperature was kept at 37 °C, within the 0.5 °C limit of the regulation system (Control and Readout Ltd.; models 302 and 204). The bottom of the chamber consists of a glass coverslip sandwiched above a wire mesh (diameter of the wire 0.05 mm, mesh width 1 mm; Rhodius, Weissenburg, Federal Republic of Germany) that is connected to the external conductor of the TEM cell. The combination of wire mesh and glass coverslip allows the use of all microscopic objectives (even those with

high apertures and smallest working distances) without disturbing the field inside the TEM cell, except for causing local inhomogeneities of the electrical field vector (see below under Dosimetry). The TEM cell is mounted on the object stage of the inverted microscope. The bottom of the TEM cell serves as part of the sliding object stage of the microscope, allowing controlled displacement of the TEM cell.

2.4 Dosimetry

To determine the specific absorption rate (SAR) value, a combination of measurements and computation was used. The following were steps taken to obtain the SAR value. 1) We measured ϵ_r (relative dielectric constant), μ_r (relative magnetic permeability), ρ (conductivity) of the medium (Tyrode's solution), and the polyacryl-glass of the experimental chamber. At a frequency of 900 MHz, the following values were obtained: Tyrode's solution, $\epsilon_r = 70$ and $\rho = 1.5$ S/m; for comparison: distilled water, $\epsilon_r = 81$, $\rho = 0$ S/m; whole blood, $\epsilon_r = 63$, $\rho = 1.25$ S/m (blood values measured by V. Anderson; Telstra, Australia); and polyacryl, $\epsilon_r = 2.3$,

$\rho = 0$ S/m. All values for μ_r are 1. In addition, the specific weight of Tyrode's solution was found to be 1,004.09 g/liter. 2) Numerical modelling was carried out of the geometry of the TEM cell and the experimental chamber consisting of the polyacryl-glass body (cylinder with a concentric hole) and the probe volume (cylinder of Tyrode's solution). The dimensions of these two cylinders in the middle of the bottom of the TEM cell are given in Figure 2. 3) Calculation of the electrical field distribution in the whole interior of the TEM cell was based on the measured material constants. The computation shows that the electrical field strength in Tyrode's solution decreases to 1/54 of the value in the empty experimental chamber, whereas the magnetic field strength remains nearly the same. 4) The power (P_{Joule}) deposited in the probe volume was calculated by the equation

$$P_{\text{Joule}} = \int E^2 \cdot \rho dV \quad (1)$$

with reference to the field distribution in the Tyrode's solution volume (integration of all voxels in the Tyrode's solution volume for $P = 1$ W; E is the electrical field inside the solution in the probe volume; see Table 1).

Parameter	Empty TEM cell		In the solution inside the TEM cell	
	900	1,800	900	1,800
Frequency (MHz)	900	1,800	900	1,800
E (V/m)	170	170	3.13	4.92
B (μ T)	0.563	0.566	0.626	0.778
S (W/m ²)	76.2	76.6	1.56	3.05
SAR (mW/kg)	-	-	11	34.4

Table 1. High-Frequency Field Parameters Within the TEM Cell at 1 W Input Power

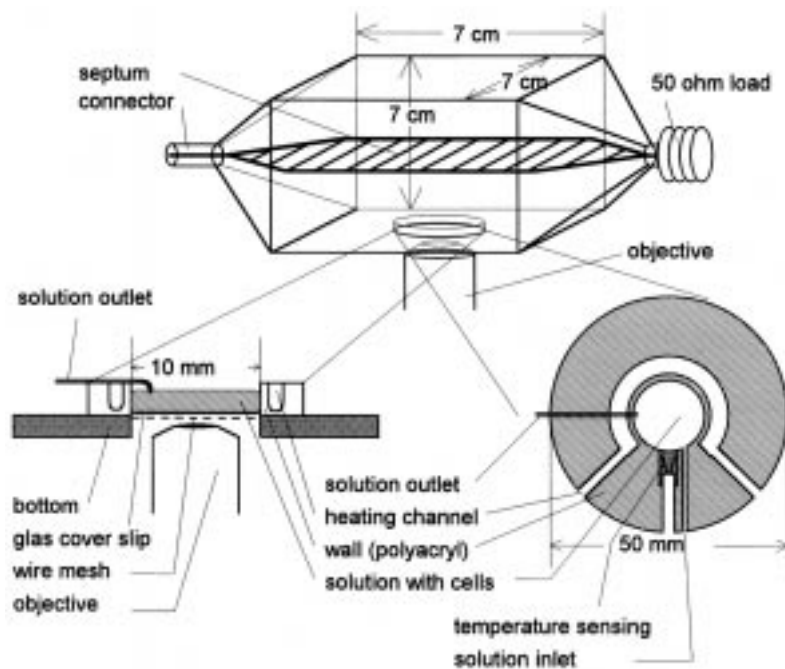


Fig. 2. Transversal-electromagnetic (TEM) cell and the experimental chamber. The TEM cell is mounted on the object stage of an inverted microscope with the open experimental chamber on the inside of the bottom. The experimental chamber consists of a round polyacryl body with a central hole of 10 mm diameter forming the probe volume. The probe volume is open at the top and closed at the bottom by a glass coverslip over a wire mesh connected to the external conductor of the TEM cell. Permanent perfusion is performed via a solution inlet and outlet. Temperature is kept constant by a temperature-sensing device coupled to a system pumping heated liquid through a channel around the probe volume and a heat exchanger for prewarming the perfusion solution.

All calculated SAR values, power densities, and numerical values of the electric and magnetic fields at 900 MHz and 1,800 MHz for the empty TEM cell and with Tyrode's solution in the probe volume are listed in Table 1.

From the calculated numerical values of E and B , the power density $s = E \times H$ can be calculated using $\mu_r = 1$ and $E \perp H$ as follows: $s = E \cdot B/\mu_0$ ($\mu_0 = 1.256 \cdot 10^{-6}$ Vs/Am). The SAR values were calculated with Equation 1. Two SAR values were calculated for each pulsed application pattern, one as mean SAR value (SAR_{mean}) and one for the peak pulse power (SAR_{peak}). The TEM cell input

power was measured for each application pattern with a bolometer (tft-powermeter, type 6460/1; Marconi, Stevenage, U.K.). Multiplication of the SAR values in Table 1 with the measured input powers gave the SAR values listed in Table 2. SAR_{mean} was transformed to SAR_{peak} according to the assumption that all power was emitted during the pulse duration. The calculated SAR values are mean values within the solution.

Because the experimental chamber was part of the TEM cell, the field strength inside the solution was not even. The bottom of the experimental chamber, as men-

tioned above, consists of a glass coverslip on a wire mesh. The wire mesh below the coverslip closes the TEM cell for the high-frequency fields. The field lines converge to the wires, causing local inhomogeneities of the SAR values, i.e., close to the wires, the SAR value is higher, and, in the center of a mesh, the SAR value is lower than stated. According to calculations made by Prof. Dr. V. Hansen using the computer program MAFIA at the Institute for Theoretical Electrotechnique (University of Wuppertal, Wuppertal, Federal Republic of Germany), local SAR values may vary by one order of magnitude around the values in Table 2 depending on the position of an individual cell in the experimental chamber. One millimeter above the wire mesh, the field distribution is even.

If the local variations of the SAR values are taken into account, then cells that lie in the center of a mesh will absorb as much or little more energy than cells in $^{45}\text{Ca}^{2+}$ efflux studies with lower carrier frequencies: neuronal tissue at 50 MHz, 147 MHz, 450 MHz, 0.5 mW/kg, 0.6 mW/kg, 1.3 mW/kg [Adey, 1980]; Blackman et al., 1980a,b (SAR values given by Schwartz et al. [1990]) and 0.27–5.29 mW/kg [Blackman et al., 1989]; whole heart muscle at 240 MHz, 0.15 mW/kg, and 0.3 mW/kg [Schwartz et al., 1990]. Cells lying close to the wires will absorb as much energy (50 mW/kg) as neuronal tissue in the experiments of Dutta et al. [1984]. All of the studies cited used sinusoidally modulated radiofrequency (RF) fields, whereas, in this study, square-wave modulation (rise time 2.5 μs) was applied.

2.5 Experimental Design and Tested Parameters

Each experimental run consisted of three phases (duration 500 s each). Phase 1, without any field application or chemical stimulation, was followed by field exposure in phase 2. During phase 3, the field was switched off, and a chemical stimulation was performed by application of a solution containing 135 mM KCl instead of NaCl, which served as positive control (Fig. 1). The high- K^+ /low- Na^+ solution depolarizes the membrane potential to about 0 mV, thus, causing an increase in $[Ca^{2+}]_i$.

The experimental schedule contained three main variations of parameters, carrier frequency, modulation frequency, and membrane potential. The carrier frequency was varied in three steps (900, 1,300, and 1,800 MHz), including the two frequencies relevant for mobile communication

(e.g., GSM standard). At 900 MHz, the modulation frequency was varied over a wide range: continuous wave (CW), 16 Hz, 50 Hz, 217 Hz, and 30 kHz, which was the maximal modulation frequency practicable by our equipment. The waveform for this modulation was rectangular with 100% modulation amplitude, and the duty cycle was 50% for 16 Hz and 50 Hz, 14% for 217 Hz (reproducing the pulse pattern of mobile communication devices following the GSM standard), and 80% for 30 kHz. The experiments included sham runs without field exposure but with the same handling of the cells and the same duration of experiments.

In one set of experiments, the membrane potential of the cells was adjusted to different values (the approximate values are given in Table 3). In phase 3, the membrane potential of the depolarized cells was repolarized to -80 mV. This set also included sham

runs at each membrane potential.

In a third set of experiments, long-term exposures were tested. Phase I (without field) was 5 min duration and was followed by 120 min of exposure (phase 2) and 25 min of chemical stimulation without field (phase 3). These experiments were compared to long-term sham runs.

2.6 Evaluation Procedures

To evaluate the behavior of the cells under the influence of the high-frequency field and chemical stimulation, we defined two values to characterize the reaction of each cell. Assuming an accumulating RF effect, only ratios at the end of an interval were evaluated.

In a first step, the average value of ten ratio values corresponding to the $[Ca^{2+}]_i$ between 400 and 490 s was calculated (x_i , character-

Carrier freq. (MHz)	Mod. freq. (Hz)	Pulse (%)	SAR _{mean} (mW/kg)	SAR _{peak} (mW/kg)	Number of cells	$d_1 \pm S.D.$	$d_2 \pm S.D.$	T value ($d_1/sham$)
Exposure time, 500 s								
Sham	-	-	-	-	55	0.011 ± 0.014	0.213 ± 0.111	-
900	Cont.	-	59	59	42	0.013 ± 0.009	0.207 ± 0.073	0.81
900	16	50	29	57	30	0.005 ± 0.013	0.193 ± 0.092	-1.94
900	50	50	30	59	40	0.001 ± 0.009	0.197 ± 0.091	-3.96
900	217	14	15	123	39	0.005 ± 0.031	0.159 ± 0.078	-1.27
900	30,000	80	37	47	39	0.005 ± 0.006	0.147 ± 0.035	-2.51
1,300	217	14	12	99	32	0.007 ± 0.009	0.178 ± 0.066	-1.45
1,800	217	14	9	69	37	0.008 ± 0.009	0.178 ± 0.006	-1.15
Exposure time, 120 min (7,200 s)								
Sham	-	-	-	-	33	-0.025 ± 0.039	0.205 ± 0.08	-
900	217	14	15	123	47	-0.012 ± 0.018	0.204 ± 0.07	-2.00

Table 2. Results of the Experiments Carried Out at Resting Potentials*

*Specific absorption rate (SAR)_{mean} and SAR_{peak} are average values over all cells.

The SAR value for one individual cell may vary plus or minus a factor of 3 around the values stated here.

3. Results



Overall view on the experimental set-up with its different components.

During this study, $[Ca^{2+}]_i$ in more than 600 heart muscle cells was measured. The $[Ca^{2+}]_i$ was calibrated in some representative experiments ($n = 61$ cells). The concentration in resting cells was 154 ± 20 nM (mean \pm S.D.). This concentration remained stable throughout an experiment of 120 min duration. After this time, the cells still responded to a depolarization with 135 mM KCl, resulting in a membrane potential shift to about 0 mV with an increase in $[Ca^{2+}]_i$. In the mean of all calibrated cells (short- and long-term experiments), the $[Ca^{2+}]_i$ rose to 523 ± 58 nM during the K^+ depolarization to 0 mV. The K^+ depolarization served as a viability test and a demonstration of working Ca^{2+} transport mechanisms in the cells. This behavior of the cells is exhibited in Figure 1 in the plot of the $[Ca^{2+}]_i$ of a single cell as a function of time.

Sometimes, the ratio values during long-term experiments declined throughout the observation time. This may be due to various mechanisms. Because we

izing phase 1; Fig. 1). A second value, the mean of the ratio values between 900 and 990 s (x_2 characterizing phase 2), and a third value, the mean of the ratio values between 1200 and 1290 s (x_3 characterizing phase 3), were calculated for comparison. The difference between x_2 and x_1 (d_1) is characteristic of the influence of the electromagnetic field on the measured ratio, and the dif-

ference between x_3 and x_2 (d_2) gives a measure of the effect of the chemical stimulation after high-frequency application. For each experimental situation, the average and standard deviation of d_1 and d_2 for all cells were computed. The d_1 values of sham-exposed samples were compared to the values of the exposed samples by an unpaired, double-sided Student's t test.

$U_{approx.}$ (mV)	Treatment	KCl (mM)	NaCl (mM)	n	$d_1 \pm$ S.D.	$d_2 \pm$ S.D.	T values ($d_1/sham$)
-80	Sham	4	135	55	0.011 ± 0.014	0.213 ± 0.111	-1.27
-80	Exposed	4	135	39	0.005 ± 0.031	0.159 ± 0.078	
-50	Sham	20.4	118.6	40	0.012 ± 0.016	0.005 ± 0.015	1.523
-50	Exposed	20.4	118.6	31	0.007 ± 0.01	-0.006 ± 0.01	
-30	Sham	43.5	95.5	34	-0.011 ± 0.055	-0.032 ± 0.025	-1.865
-30	Exposed	43.5	95.5	37	0.006 ± 0.007	-0.025 ± 0.022	
0	Sham	135	0	34	-0.013 ± 0.018	-0.136 ± 0.086	-0.764
0	Exposed	135	0	31	0.010 ± 0.013	-0.133 ± 0.037	

Table 3. Results of the Experiments Carried Out at Various Potentials

Results

did not block the anion transport by probenecid, it is possible that fura-2 was removed from the cytoplasmic matrix by sequestration within intracellular compartments or by secretion into the extracellular solution, which has been seen in many other cell types [Di Virgilio et al., 1990]. In addition, the dye may bleach throughout the experiment or may be degraded [Becker and Fay, 1987]. All mechanisms will decrease the sensitive dye concentration. Because the fura-2 ratio is not completely independent of the dye concentration, this can cause smaller ratio values. Because the decrease of ratio values is a nonrandom event, the averaged d_1 values in these "long-term" experiments are below 0: $d_1 = -0.0252 \pm 0.0386$; $n = 33$ for sham exposures. The d_2 value in the same series was 0.2053 ± 0.08 .

An exposure of cardiocytes to 900 MHz modulated by 217 Hz between 5 and 125 min after the start of the experiment did not result in significantly diverging d values: $d_1 = -0.0118 \pm 0.0181$; $d_2 = 0.2038 \pm 0.07$ ($n = 47$). The

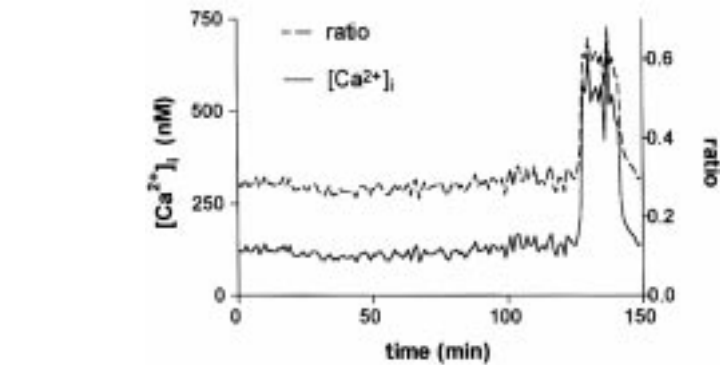


Fig. 3. Ratio and intracellular calcium concentration ($[Ca^{2+}]_i$) plotted vs. time for a long-term experiment. The cell concerned shows a stable $[Ca^{2+}]_i$ around 100 nM during the experiment (sham exposure) and fluctuations of the $[Ca^{2+}]_i$ during chemical stimulation.

t value (double sided, unpaired) for the comparison of the d_1 values was -2.00 . Accordingly, the two d_1 values are not different at 1% probability limit. Both d_2 values exhibit a relatively high standard deviation compared to the d_1 values. This is due to normal differences in the increase of $[Ca^{2+}]_i$ during potassium depolarization and to fluctuations in $[Ca^{2+}]_i$ during this time (Fig. 3). Some cells develop $[Ca^{2+}]_i$ waves or oscillations when they are depolarized to 0 mV. Although the

frequency of these waves cannot be resolved because of the low rate of image acquisition, this behavior is monitored as fluctuations of the $[Ca^{2+}]_i$.

The standard experiments lasted shorter (1,500 s long) and the frequency of image acquisition was higher (0.1 Hz) than in the long-term exposure experiments. In the standard experiments, the carrier frequency as well as the pulsation pattern were varied over a wide range. An original recording of one cell is exhibited in Figure 1. The results of these experiments are not discussed in detail, because they do not differ fundamentally from those of long-term exposures. A steady decrease in fluorescence intensity is not visible in the standard experiments due to their shorter duration. The results of both the long- and short-term experiments are compiled in Figure 4 and in Table 2. In Figure 4, the d_1 and d_2 values are plotted. All d_2 values are well above the d_1 values (≈ 0.2 ratio values). Because the standard deviations of the corresponding d_1 and d_2 values do not overlap,

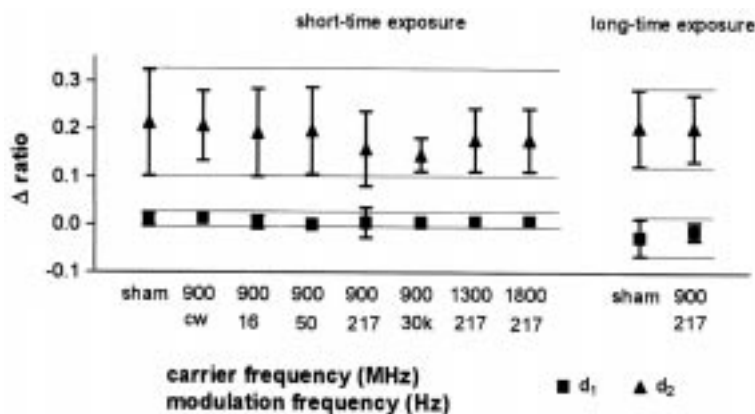


Fig. 4. Plot of d_1 and d_2 vs. the exposure pattern. Each d value is plotted with its standard deviation. For comparison, the standard deviation of the sham exposure is marked by horizontal lines.

it is obvious that the chemical stimulation worked well in all cases. A comparison of the d_1 values of the different exposure patterns reveals that they are all within the limits of the standard deviation of the sham exposures. Nevertheless, the t test revealed a difference at 1% probability limit for the 900 MHz/50 Hz pulsation pattern. However, we do not think that this difference represents an influence of the field exposure, because the measured mean value lies within the limits of the standard deviation of the sham exposure and lies even closer to the expected ideal value of 0 for d_1 than any other value. Comparison of the d_2 values of exposed cells to those of sham-exposed cells does not indicate any influence of the high-frequency field on the subsequent ability of the cells to take up high amounts of Ca^{2+} and to pump it out again.

The ability of the cells to handle higher loads of Ca^{2+} in the presence of a high-frequency electromagnetic field was checked in the set of experiments in which the membrane potential was depolarized. The potential was depolarized to about -50, -30, and 0 mV during phase 1 in the absence of the field. Ten seconds after the start of the experiment, the perfusion was changed to a medium containing high K^+ and low Na^+ ; it was switched back to standard Tyrode's solution 1,000 s after the start. It usually took ≈ 100 s until the perfusing medium was completely replaced by a new one. Because the field was switched on 500 s after the onset of the experiment and switched off again 500 s later, the exposure started while the cells were de-

polarized and ended before the cells had repolarized. In these experiments, we exclusively applied fields of 900 MHz and 217 Hz with the SAR value listed in Table 2. The $[\text{Ca}^{2+}]_i$ rose only when the potential was depolar-

ized to -30 and 0 mV (Fig. 5). In these cases, the $[\text{Ca}^{2+}]_i$ remained high as long as the cells were depolarized. The d_1 and d_2 values of exposed cells were compared to values of cells depolarized in the same way but in the absence of a

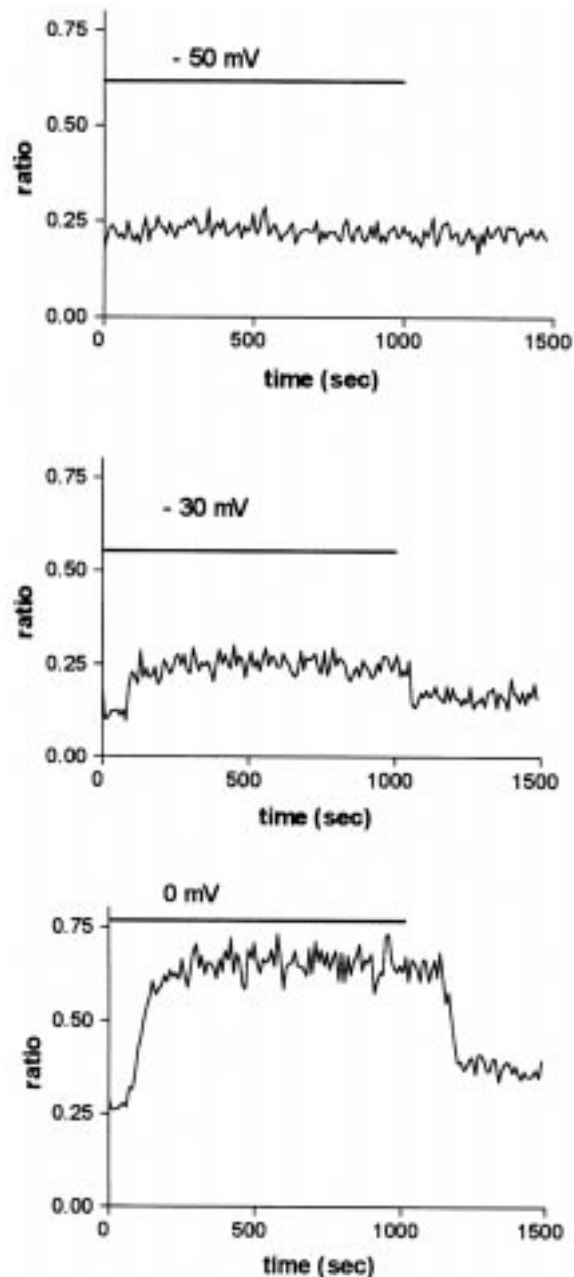


Fig. 5. Ratio plotted vs. time for different membrane potentials. The membrane potentials mentioned were adjusted by application of adequate extracellular media during the time periods indicated by the horizontal lines.

high-frequency field. The d_2 value of the cells in these experiments was the difference between the average ratios from the cells in the depolarized and the repolarized state. The d_1 and d_2 values are listed in Table 3. For comparison, the d values of the resting potential from Table 2 are also listed in Table 3 (-80 mV line). Because the depolarization to -50 mV did not influence the $[Ca^{2+}]_i$, the repolarization was also without any effect (Fig. 5), and the d_2 values are in the range of zero. In the case of depolarization to -30 mV, a small but clearly visible rise in the $[Ca^{2+}]_i$ was induced (Fig. 5). Thus, the repolarization decreased the $[Ca^{2+}]_i$ again, and slightly negative d_2 values were calculated. Depolarization to 0 mV (used as chemical stimulation in the experiments listed in Table 2) caused a clear rise in $[Ca^{2+}]_i$ in these experiments as well, and repolarization induced full restoration of the low $[Ca^{2+}]_i$, leading to clearly negative d_2 values.

4. Discussion

For the on-line measurement of $[Ca^{2+}]_i$ during application of high-frequency fields, a setup for microscopic observation was developed. The high-frequency fields were applied in a specially designed TEM cell, which has a "window" at the bottom that allows visual access to the specimen. TEM cells have been used as exposure systems in many earlier studies dealing with Ca^{2+} homeostasis [Blackman et al., 1979, 1989; Dutta et al., 1984, 1989; Schwartz et al., 1990]. Thus, the exposure system, although it was

especially adapted for use on a microscope, produces field configurations comparable to those of earlier investigations. In contrast to these earlier studies, the position of the sample was practically on the TEM cell wall. This is necessary for the use of objectives with short working distances for microscopic observations. One disadvantage of this configuration is the larger range of power densities caused by the close position to the wire mesh (see above under Dosimetry).

The main aim of this study was to test whether, at athermal energies, the frequency and pulse patterns emitted from modern digital wireless telecommunication devices influence the $[Ca^{2+}]_i$ in excitable cells. Other pulse patterns that are near the "frequency windows" demonstrated in efflux studies were also included in this study in order to determine whether there is an influence on the $[Ca^{2+}]_i$ in these cases. To our knowledge, carrier frequencies around 1 GHz were applied in only two $^{45}Ca^{2+}$ efflux studies: 915 MHz [Dutta et al., 1984] and 1 GHz [Schwartz and Mealing, 1993]. Both studies screened a wide variety of SAR values in the athermal energy range at 16 Hz sinusoidal modulation. Whereas the work of Schwartz and Mealing [1993] failed to demonstrate any effect on Ca^{2+} efflux and contraction of frog atrial muscle, Dutta et al. [1984] demonstrated a clearly increased efflux rate from human neuroblastoma cells irradiated with 915 MHz sinusoidally modulated at 16 Hz with an SAR value of 50 mW/kg. They observed an increase in the $^{45}Ca^{2+}$ efflux rate of around 50%, which must be judged as a big effect.

The mean SAR value of ≈ 30 mW/kg applied in our study using 900 MHz square-wave modulated with 16 Hz is close to their effective value. Nevertheless, the measurements presented in our study do not reveal any clear effect of the applied fields on the $[Ca^{2+}]_i$ of isolated ventricular heart muscle cells of the guinea pig. In only one case (900 MHz/50 Hz), a small but significant difference between the sham-exposed and exposed cells was demonstrated. Because the average value of the exposed cells is still within the limits of the standard deviation of the sham-exposed cells, and because the difference is that small, we conclude that this must not be judged to be a relevant difference caused by the field.

An effect at an unknown energy window might have been missed during this study, because the SAR values have not been varied systematically. Energy windows in the athermal energy range have been reported by Blackman et al. [1989]. At several energies below 5.29 mW/kg, they demonstrated an enhanced efflux of $^{45}Ca^{2+}$ from chicken brain caused by 50 MHz fields sinusoidally modulated with 16 Hz. Compared to the SAR values reached in this study at 16 Hz square-wave modulation, those of Blackman et al. [1989] were lower. In our cases of comparable low SAR values, the carrier frequency and the pulse pattern differed from those of Blackman et al. [1989].

The finding that the $[Ca^{2+}]_i$ in ventricular myocytes of the guinea pig are not influenced by pulsed high-frequency fields seems to be in contrast to the results of the $^{45}Ca^{2+}$ efflux studies on neuronal

tissue and cells [Bawin et al., 1975, 1978; Blackman et al., 1979, 1989; Lin-Liu and Adey, 1982; Dutta et al., 1984, 1989] and heart tissue [Schwartz et al., 1990], but this is not necessarily the case. In most of those experiments, the carrier frequency was below 500 MHz, which is a difference between the present study and those studies. In a $^{45}\text{Ca}^{2+}$ efflux study, Schwartz et al. [1990] demonstrated an increased efflux from whole frog hearts due to irradiation with 240 MHz fields modulated sinusoidally with 16 Hz at low SAR values of 0.15 and 0.3 mW/kg. Their findings are in very good agreement with the results obtained on neuronal tissue and cells. The study of Schwartz and Mealing [1993], who used a carrier frequency (1 GHz) in the same range as the frequencies tested here, did not demonstrate any influence of the field either on the $^{45}\text{Ca}^{2+}$ efflux or on the contraction of the frog atrial strips. Especially, their finding that the amplitude of contraction was not influenced is in line with our measurements of $[\text{Ca}^{2+}]_i$, because the amplitude of contraction depends directly on the $[\text{Ca}^{2+}]_i$. However, our measurements were carried out on resting cells and on cells in the state of K^+ depolarization and not on paced cells, which means that a possible influence on the excited heart cell might have been hidden in the experiments of our study.

Additionally, there is a basic difference between measurements of the $[\text{Ca}^{2+}]_i$ and the $^{45}\text{Ca}^{2+}$ efflux. The measurement of the $[\text{Ca}^{2+}]_i$ demonstrates with relatively high precision the Ca^{2+} concentration in the cytoplasm of the cell. This concentration can be influenced by various causes, such as Ca^{2+}

being exchanged between the cytoplasm and intracellular Ca^{2+} stores or Ca^{2+} exchange between the extracellular space and the cytoplasm. The $^{45}\text{Ca}^{2+}$ efflux measurements, on the other hand, summarize the whole exchange of Ca^{2+} between the cells or the tissue and the solution in the extracellular space. There are two sources of exchange with the extracellular solution: Ca^{2+} being exchanged across the cell membrane between cytoplasm and the external solution and Ca^{2+} being exchanged between the binding sites on the external surface of the membrane and the external solution. Thus, a change in the amount of Ca^{2+} bound to the external surface of the membrane will be visible in $^{45}\text{Ca}^{2+}$ efflux measurements but not necessarily in measurements of $[\text{Ca}^{2+}]_i$. Nevertheless, changes of the amount of Ca^{2+} bound to the external surface of the membrane will influence the gating behavior of membrane channels and, thus, the $[\text{Ca}^{2+}]_i$ (at least of regularly excited cells). An influence of the high-frequency fields on the Ca^{2+} bound to the external surface of the cells might have been overlooked in the present experiments because the cells were not paced.

Because most of the $^{45}\text{Ca}^{2+}$ efflux measurements are based on the pioneering work of Bawin et al. [1975], they were also carried out on neuronal cells. The interpretation of the results was that the amount of Ca^{2+} bound to the external surface is affected by the high-frequency fields [Adey, 1990]. Taking this interpretation into account, there are four possible reasons for the negative results revealed in this study. 1) Mammalian heart muscle cells are

less sensitive to high-frequency fields than neuronal cells. 2) The cells' reactions depend not only on the modulation frequency but also on the pulsation pattern (sine-wave modulation or square-wave modulation). 3) Either the tested carrier frequency was too high to induce any changes or changes appear at an energy window not tested in this study. The existence of multiple power-density windows as reported by Blackman et al. [1989] has not been tested systematically. 4) Only the Ca^{2+} bound to the external surface of the membrane is influenced by the high-frequency fields, and this has not influenced the $[\text{Ca}^{2+}]_i$ under the experimental conditions of this study.

The SAR values applied in this study are in the athermal range; thus, they are clearly below values that can be reached in the brains of mobile phone users. Values between 1 and 2 W/kg [Lovisol et al., 1995] and between 0.1 and 0.3 W/kg [Gajda and Thansandote, 1995] are discussed for this situation. Nevertheless, the SAR values in this study represent the exposure range for people living around radio stations for wireless telecommunication.

Although this study does not exclude an influence of pulsed high-frequency fields in the range between 900 and 1,800 MHz on the $[\text{Ca}^{2+}]_i$ of ventricular myocytes, it makes such influence less probable. Experiments in progress on stimulated heart muscle cells using the patch-clamp technique will elucidate the possible influence of pulsed high-frequency fields on the cell membrane more clearly.

5. Acknowledgements

We thank Prof. Dr. V. Hansen for his help with the calculations of the SAR values. This study was supported by the Forschungsverbund Braunschweig and by the Forschungsgemeinschaft Funk (Bonn, Federal Republic of Germany).

6. References

- Achenbach C, Wiemer J, Preissler R (1985): Isolation of adult ventricular myocytes for electrophysiological experiments [abstract]. In Piper HM, Spieckermann PG (eds): "Adult Heart Muscle Cells." Darmstadt: Steinkopff-Verlag, pp 13–17.
- Adey WR (1980): Frequency and power windowing in tissue interactions with weak electromagnetic fields. *Proc IEEE* 69:119–125.
- Adey WR (1990): Electromagnetic fields and the essence of living systems. In Andersen JB (ed): "Modern Radio Science." Oxford: Oxford University Press, pp 1–36.
- Bawin SM, Kaczmarek LK, Adey WR (1975): Effects of modulated VHF fields on the central nervous system. *Ann NY Acad Sci* 247:74–81.
- Bawin SM, Sheppard AR, Adey WR (1978): Possible mechanisms of weak electromagnetic field coupling in brain tissue. *Bioelectrochem Bioenerg* 5:67–76.
- Becker PL, Fay FS (1987): Photo-bleaching of fura-2 and its effect on determination of calcium concentrations. *Am J Physiol* 22:C613–C618.
- Berridge MJ (1993): Inositol trisphosphate and calcium signaling. *Nature* 361:315–325.
- Blackman CF, Elder JA, Weil CM, Benane SG, Eichinger DC, House DE (1979): Induction of calcium-ion efflux from brain tissue by radiofrequency radiation: Effect of modulation frequency and field strength. *Radio Sci* 14:93–98.
- Blackman CF, Benane SG, Elder JA, House DE, Lampe JA, Faulk JM (1980a): Induction of calcium-ion efflux from brain tissue by radiofrequency radiation: Effect of sample number and modulation frequency on the power density-window. *Bioelectromagnetics* 1:35–43.
- Blackman CF, Benane SG, Joines WT, Hollis MA, House DE (1980b): Calcium-ion efflux from brain tissue: Power-density vs. internal field-intensity dependencies at 50-MHz RF radiation. *Bioelectromagnetics* 1:277–283.
- Blackman CF, Kinney LS, House DE, Joines WT (1989): Multiple power density windows and their possible origin. *Bioelectromagnetics* 10:115–128.
- Blatter LA, Wier WG (1994): Nitric oxide decreases $[Ca^{2+}]_i$ in vascular smooth muscle by inhibition of the calcium current. *Cell Calcium* 15:122–131.
- Carafoli E (1987): Intracellular calcium homeostasis. *Annu Rev Biochem* 56:395–433.
- Clapham DE (1995): Calcium signaling. *Cell* 80:259–268

- Di Virgilio F, Steinberg TH Silverstein SC (1990): Inhibition of fura-2 sequestration and secretion with organic anion transport blockers. *Cell Calcium* 11:57–62.
- Dutta SK, Subramoniam A, Ghosh B, Parshad R (1984): Microwave radiation-induced calcium ion efflux from human neuroblastoma cells in culture. *Bioelectromagnetics* 5:71–78.
- Dutta SK, Ghosh B, Blackman CF (1989): Radiofrequency radiation-induced calcium ion efflux enhancement from human and other neuroblastoma cells in culture. *Bioelectromagnetics* 10:197–202.
- Fabiato A (1988): Computer programs for calculating total from specified free or free from specified total ionic concentrations in aqueous solutions containing multiple metals and ligands. In Fleischer S, Fleischer B (eds): "Methods in Enzymology, Biomembranes, Vol 157." New York: Academic Press, pp 378–417.
- Gajda G, Thansandote A (1995): An experimental system for spatial RF dosimetric measurements. In: Abstract Book, 17th BEMS Meeting, Boston. p 148.
- Gollnick F, Meyer R, Stockem W (1991): Visualization and measurement of calcium transients in *Amoeba proteus* by fura-2 fluorescence. *Eur J Cell Biol* 55:262–271.
- Grynkiewicz G, Poenie M, Tsien RY (1985): A new generation of Ca²⁺-indicators with greatly improved fluorescence properties. *J Biol Chem* 260:3440–3450.
- Kullnick U (1992): Influence of weak nonthermic high-frequency electromagnetic fields on the resting potential of nerve cells. *Bioelectrochem Bioenerg* 27:293–304.
- Lin-Liu S, Adey WR (1982): Low-frequency, amplitude-modulated microwave fields change calcium efflux rates from synaptosomes. *Bioelectromagnetics* 3:309–322.
- Lovisollo GA, Guelfi M, Bardati F, Marrocco G, Tognolatti P (1995): Experimental measurements and calculations for defining reference standard conditions of mobile communication compliance test. In: Abstract Book, 17th BEMS Meeting, Boston. p 104.
- Miura M, Okada J (1991): Non-thermal vasodilatation by radio frequency burst-type electromagnetic field radiation in the frog. *J Physiol* 435:257–273.
- Miura M, Takayama K, Okada J (1993): Increase of nitric oxide and cyclic GMP of rat cerebellum by radio frequency burst-type electromagnetic field radiation. *J Physiol* 461:513–524.
- Pozzan T, Rizzuto R, Volpe P, Meldolesi J (1994): Molecular and cellular physiology of intracellular calcium stores. *Physiol Rev* 74:595–636.
- Schwartz JL, Mealing GA (1993): Calcium-ion movements and contractility in atrial strips of frog heart are not affected by low-frequency-modulated, 1 GHz electromagnetic radiation. *Bioelectromagnetics* 14:521–533.
- Schwartz JL, House DE, Mealing GA (1990): Exposure of frog hearts to CW or amplitude-modulated VHF fields: Selective efflux of calcium ions at 16 Hz. *Bioelectromagnetics* 11:349–358.
- Stegemann M, Meyer R, Haas HG, Robert-Nicoud M (1990): The cell surface of isolated cardiac myocytes: A light microscope study with use of fluorochrome-coupled lectins. *J Mol Cell Cardiol* 22:787–803.
- Tarricone L, Cito C, D'Inzeo D (1993): Ach receptor channel's interaction with MW fields. *Bioelectrochem Bioenerg* 30:275–285.



Imprint

Newsletter Edition Wissenschaft of the FGF e.V.

Edited by: Forschungsgemeinschaft Funk e.V., Rathausgasse 11a,
D-53113 Bonn, telephone: +49(0)228 / 72622-0, telefax: +49(0)228 / 7262211

Editor: Gerd Friedrich (responsible)

Design + Typesetting: Autoren Societät, Bonn

This study was realized on behalf of the Forschungsgemeinschaft Funk e.V.
The content of the reports is representing the authors' point of view and
not necessarily the opinion of the FGF.

ISSN 1430-1458